

# Numerical evidence for a novel superfluid-insulator transition of one-dimensional bosons in strong disorder

Susanne Pielawa<sup>1</sup> and Ehud Altman<sup>1,2</sup>

<sup>1</sup>*Department of Condensed Matter Physics, Weizmann Institute of Science, Rehovot 76100, Israel*

<sup>2</sup>*Department of Physics, University of California, Berkeley, California 94720, USA*

(Dated: August 17, 2022)

We present numerical evidence from Monte-Carlo simulations that the superfluid-insulator quantum phase transition of interacting bosons subject to strong disorder in one dimension is controlled by a novel critical point. At the critical point the distribution of superfluid stiffness over disorder realizations develops a power-law tail reflecting a universal distribution of weak links. The Luttinger parameter on the other hand does not take on a universal value at this critical point, in marked contrast to the known Berezinskii-Kosterlitz-Thouless-like superfluid-insulator transition in weakly disordered systems. We develop a finite-size scaling procedure which allows us to directly compare the numerical results from systems of linear size up to 1024 sites with theoretical predictions obtained in [PRL **93**, 150402 (2004)], using a strong disorder renormalization group approach. The data shows good agreement with the scaling expected at the strong-disorder critical point.

Superfluids at non vanishing temperature in two dimensions, or at zero temperature in one dimension, can sustain at best algebraic order [1, 2]. Establishment of algebraic order at a critical temperature, or in one dimension, at a critical value of some Hamiltonian parameter, is ubiquitously understood in terms of the Berezinskii-Kosterlitz-Thouless transition (BKT) [3, 4]. The hallmark of a BKT transition is a universal jump of the exponent associated with the algebraic decay, or Luttinger parameter, at the critical point [5, 6]. Can the transition occur through an alternative mechanism, which would give rise to a different universality class?

Systems of bosons in a disordered potential provide a good arena to investigate this question. Since both the effects of interaction and of quenched disorder are particularly strong in one dimension, the interplay between the two may well lead to new physics. In a seminal work, Giamarci and Schultz [7] addressed the localization transition of interacting bosons by starting from a clean harmonic fluid (Luttinger liquid) description and added the disorder perturbatively. This analysis predicts a BKT transition, but with a universal jump of the Luttinger parameter that is different than the clean case.

Recently an alternative paradigm for the superfluid insulator transition was proposed in a theory focusing on strong disorder [8, 9]. Analysis of the problem using strong disorder renormalization group (SDRG) predicted a transition that is controlled by rare weak links that can potentially cut the chain. In the course of renormalization to longer scales, the effective distribution of weak links flows toward a universal structure, which determines the universal behavior at the critical point. The value of the Luttinger parameter at the transition is, however, non-universal and depends where the phase boundary is crossed (i.e. on the strength of the bare disorder and interactions).

The question if the proposed critical point is actually realized remains controversial [10, 11]. This controversy

is exacerbated by the fact that while the disorder grows under the SDRG flow it does not reach an infinite value and thus the method does not become asymptotically exact as it does in other instances of random critical points [12]. It is therefore hard to rule out the possibility that even when the bare disorder is strong the critical system eventually flows to the weak disorder Giamarchi-Schulz fixed point.

A number of previous works have attempted to resolve this question numerically, but the lack of an appropriate finite-size scaling procedure did not allow to probe directly for the strong-disorder fixed point. Balabanyan *et al* [10] found relatively good agreement with the BKT transition using one type of disorder, but noted strong finite-size effects when a different disorder type was used. Hrahsheh and Vojta [13] measured a non-universal Luttinger parameter at the transition, consistent with the prediction of the SDRG, but did not look for universal signatures of the strong disorder critical point. Pollet *et al* [11] proposed a classical-field renormalization flow to explain the system's behavior, which did not match BKT scaling. These authors argued that at very long, numerically inaccessible, scales the classical flow will revert to a usual BKT transition.

In this paper we characterize the critical properties of the transition using Quantum Monte Carlo simulations of a standard bosonic model, comparing directly against universal predictions of the SDRG. The crucial new element in our analysis is the development of an appropriate finite size scaling procedure. We find good agreement with the scaling predicted by the SDRG at the random critical point. We show that even inside the superfluid phase, at strong disorder, the distribution of relevant quantities, such as the stiffness necessarily invalidates the weak disorder analysis of Giamarchi and Schultz [7]. We thus conclude that beyond a certain disorder strength the transition changes character, and is controlled by the new strong disorder fixed point.

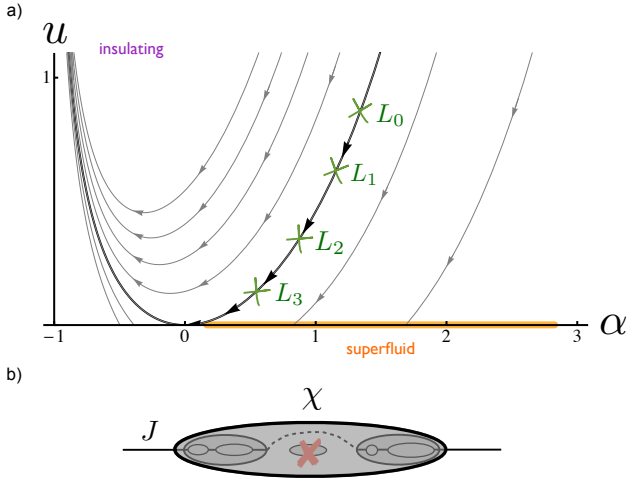


FIG. 1: a) Solutions to the flow equations near the strong-disorder fixed point. The parameter  $\alpha$  characterizes the renormalized probability distribution of weak links,  $p(J) \propto J^\alpha$ . This parameter  $\alpha$  can be extracted from numerical or experimental data via the distribution of superfluid stiffness. The parameter  $u$  describes the renormalized distribution of on-site repulsion and cannot be directly extracted from physical observables. The flow proceeds along the flow lines in the direction of the arrows, i.e. if a system starts out with bare parameters  $\alpha_0$  and  $u_0$  (point  $L_0$  in the graph) at system size  $L_1$  we will measure  $\alpha_1$ . At a larger system size  $L_2$  we will measure  $\alpha_2$ , and so on. b) The flow stops when the entire chain has shrunk to a single superfluid cluster. Here the last couple of SDRG steps are shown schematically. The last cluster has an internal stiffness  $\chi$  and is connected to itself by the last remaining link  $J$ . Both  $\chi$  and  $J$  are combined to obtain the total superfluid stiffness of the system, see Eq. (3).

*From SDRG to measurable quantities* – In order to establish the existence of a strong disorder superfluid-insulator critical point we need to identify observables, measurable in Monte Carlo simulations, that are predicted by SDRG to obey distinct universal behavior. The SDRG was carried out in Refs. 8, 9 on the following Josephson array model

$$H = \sum_i \frac{1}{2} U_i n_i^2 - J_i \cos(\theta_{i+1} - \theta_i) - \mu_i n_i, \quad (1)$$

with  $U_i$  random charging energies of grains,  $J_i$  Josephson couplings and  $\mu_i$  a random chemical potential giving rise to offset charges. For simplicity we will focus here on the case of a particle-hole symmetric model (i.e.  $\mu_i = 0$ ), however, the same analysis carried out on a model with generic disorder leads to essentially the same conclusions about the transition at strong disorder.

In the course of renormalization successive elimination of the largest couplings on the chain (1), leads to a flow

toward universal distributions of coupling constants

$$p(U) = \frac{e^U}{\Omega} \left( \frac{\Omega}{U} \right)^2 e^{-u\Omega/U} \quad (2a)$$

$$p(J) = \frac{\alpha + 1}{\Omega} \left( \frac{J}{\Omega} \right)^\alpha \quad (2b)$$

Hence in late stages of the RG the flow of full distribution functions is encapsulated in scaling equations for only two parameters  $u$  and  $\alpha$ .

The resulting flow is shown in Fig. 1. Below the separatrix the flow approaches the superfluid fixed line on the  $\alpha$  axis. The transition to the insulator occurs when the renormalized value of  $\alpha$  takes on a universal value  $\alpha = 0$ . That is, when the renormalized distribution of Josephson couplings becomes uniform. For  $\alpha < 0$  weak links become dominant and effectively cut the chain.

The essential difficulty in identifying this universal behavior in numerical simulations is that the object which becomes universal, i.e. the renormalized distribution of Josephson couplings, is a theoretical construct and not directly measurable. On the other hand averages of physical quantities, such as the superfluid stiffness  $\rho$ , compressibility  $\kappa$ , or Luttinger parameter  $K$ , take on non-universal values at the strong disorder critical point [9]. Our first task will therefore be to relate the renormalized disorder distributions with a measurable quantity. As we show below the right quantity to consider is the distribution of superfluid stiffnesses of an ensemble of realizations of the disordered chain. We argue that the tail of this distribution near  $\rho = 0$  follows a power law with the desired exponent  $\alpha$ .

This can be seen as follows. The stiffness of a chain of length  $L$  is computed by proceeding with the SDRG until the entire chain has shrunk to a single superfluid cluster. The last value of  $J$  is then the coupling of this cluster to the leads, or to itself for periodic boundary conditions. The superfluid stiffness  $\rho$  for a single disorder realization is calculated as

$$\frac{1}{\rho} = \frac{1}{L} \left( \chi + \frac{1}{J} \right), \quad (3)$$

where  $\chi = \sum_{i \in \text{cluster}} J_i^{-1}$  keeps track of the stiffness of the superfluid cluster. Here  $J_i$  are bonds that were joined to create the cluster [9]. Since  $\chi$  is integrated over the entire flow it is not universal and depends on the initial disorder. However, the largest contribution to  $1/\rho$  comes from the second part,  $J$ . This is the last link which has not yet been eliminated, and therefore it is the smallest energy scale in the system, whereas all other energy scales appearing in  $\chi$  are above the cutoff  $\Omega$  associated with the length  $L$ . Therefore, at that energy scale, the distribution of the superfluid stiffness near  $\rho \approx 0$  follows the same power law with exponent  $\alpha$  as does  $P(J)$ . For larger values of  $\rho$  the distribution becomes non-universal due

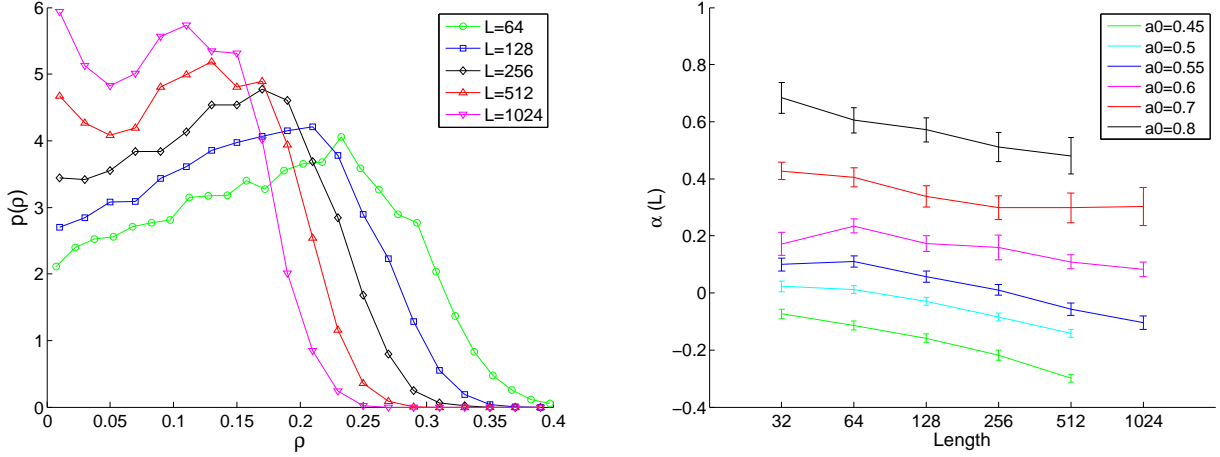


FIG. 2: a) Distribution of superfluid stiffness for  $\alpha_0 = 0.55$  for different system sizes. Near  $\rho = 0$  the distribution follows a power law, which changes as the systems size is increased. b) Values of  $\alpha$  that we extracted for different systems sizes  $L$  and initial conditions  $\alpha_0$ , on a semi-log plot. This shows that the distribution of weak links flows as the system size is increased: more weak links are generated.

to the contribution of  $\chi$ .

*Numerical simulations* – We shall perform numerical simulation of the directed loop model [10, 14], which is presumed to have the same universal properties as the Josephson array (1). This model is given in terms of the lattice action

$$S = \frac{1}{2} \sum_{\vec{n}} (K_{\vec{n}, \hat{x}} J_{\vec{n}, \hat{x}}^2 + K_{\vec{n}, \hat{\tau}} J_{\vec{n}, \hat{\tau}}^2), \quad (4)$$

where the weights are assigned according to the covering of the lattice with directed loops of currents  $J_{\vec{n}, \alpha}$  on the bonds. The integer vector  $\vec{n} = (x, \tau)$  labels the sites of the two-dimensional square lattice,  $\hat{x}$  and  $\hat{\tau}$  are unit vectors in the two lattice directions. The allowed configurations for the currents fulfill a zero-divergence constraint  $\sum_{\alpha} (J_{\vec{n}, -\alpha} + J_{\vec{n}, \alpha}) = 0$ , and by definition  $J_{\vec{n}, -\alpha} = -J_{\vec{n}-\alpha, \alpha}$ .

As usual the extra dimension of the classical model ( $\tau$  axis) stems from the imaginary time axis in the path-integral representation of the quantum partition function. Therefore the coupling constants must be uniform along that axis while they vary randomly along the  $x$  axis. These couplings can be roughly related to those of the original Josephson array model through  $K_{\tau} = U$  and  $K_x = -2 \ln(J/2)$  [10].

We take bare coupling distributions that are not far from the expected fixed point distributions in order to have fast finite size convergence to the universal regime. For the disorder in the parameter  $K_{\tau} \approx U$ , we take a distribution with  $u_0 = 0.2$ :  $p(K_{\tau}) = (e^{u_0}/K_{\tau}^2) e^{-u_0/K_{\tau}}$  for  $0 < K_{\tau} < 1$ . The bare-disorder distribution for the parameter  $K_x$  is taken as  $p(K_x) = 2^{\alpha_0}(\alpha_0 + 1)e^{-(\alpha_0+1)K_x/2}$  for  $K_x > 2 \ln 2$ . By change of variable this is a power-law

distribution for the Josephson coupling  $J$  with a power  $\alpha_0$  used here as the tuning parameter of the transition.

We performed Monte Carlo simulations of the model (4) using a classical worm algorithm [15]. For each disorder realization we computed the stiffness  $\rho_x$  [20] and constructed a full distribution from a set of 3000 to 20000 disorder realizations for each value of  $\alpha_0$  and system length  $L$  [21]. To obtain the renormalized value of  $\alpha(L)$  we extracted the exponent of the power law at the tail of the distribution at small  $\rho$  using a maximum-likelihood estimator [16].

The results of this calculation are presented in Fig. 2. First, Fig. 2(a) shows the stiffness distributions obtained for one value of the bare disorder  $\alpha_0$  and varying system sizes. In this case it is clear that the power associated with the tail of the distribution flows from slightly positive value to a negative one, i.e. to a diverging probability density at  $\rho = 0$ . Fig. 2(b) shows the change of the exponent  $\alpha$  with  $L$  for varying values of the tuning parameter  $\alpha_0$ . The error bars for  $\alpha$  shown on the plot stem from two independent sources: a) the QMC error due to limited simulation time; it is obtained by creating data sets of values for  $\rho$  shifted within their QMC error bars, then recalculating  $\alpha$ . b) An error due to limited number of disorder realizations; this error is estimated as described in Ref. 16.

At this point we can already make a few interesting observations about the transition. First, note that the tail of the stiffness distribution ubiquitously flows with system size  $L$ , giving rise to a power-law tail with an exponent  $\alpha$  that decreases monotonically with  $L$ . Within the SDRG this is understood as being due to renormalization of the Josephson coupling on eliminating sites with large

charging energy. Hence, while the flow of average stiffness may appear to be approximately classical [11], the flow of the full distribution and in particular its tail has an important quantum contribution. The second observation is that even in the superfluid phase the superfluid stiffness retains a power-law distribution near  $\rho = 0$  with exponent  $\alpha < 1$ . Consequently the variance of  $1/\rho$  diverges in this regime. This has important implications because a finite variance of  $1/\rho$  is required to obtain a dual description in terms of phase slip variables as a starting point of a weak disorder analysis [7]. Hence the numerically obtained stiffness distributions can by themselves explain the breakdown of the weak disorder theory.

*Finite-size scaling* – To quantitatively assess the agreement between the numerical data and the universal behavior expected in the vicinity of the strong disorder critical point [8, 9] we need an appropriate finite size scaling scheme. The SDRG flow takes place in the space of the two parameters  $\alpha$  and  $u$  associated with the renormalized distributions of Josephson couplings and charging energies respectively. Only one of those parameters,  $\alpha$ , can be extracted from the numerical data. But, as we show below, this gives us sufficient information to formulate a finite size scaling scheme.

The essential idea is similar to a finite size scaling procedure developed for the BKT critical point, where the RG operates in the space of stiffness and vortex fugacity, with only the stiffness being a directly measurable quantity. As a preparatory step we solve the scaling equations given in Ref. 8 to obtain flow lines  $u(\alpha, c)$ , plotted in Fig. 1. Here  $c$  is an integration constant which labels the flow lines. Next we bring the scaling equations to integral form

$$-\int_{\alpha_2}^{\alpha_1} \frac{1}{u(\alpha, c)} d\alpha - \log\left(\frac{\alpha_1 + 1}{\alpha_2 + 1}\right) + \log\left(\frac{L_2}{L_1}\right) = 0 \quad (5)$$

where  $\alpha_1$  ( $\alpha_2$ ) is the measured value at length  $L_1$  ( $L_2$ ). There is then only one unknown in the above equation: the parameter  $c$  which labels the flow lines.

Our finite-size scaling proceeds as follows: for each system size  $L_i$  we measure  $\alpha_i$ . For each pair of system sizes  $L_i$  and  $L_j$  we solve Eq. (5) numerically for the parameter  $c$ . This tells us on which flow line, and thus in which phase, the system is:  $c > 0$  corresponds to the insulating phase, and  $c < 0$  to the superfluid phase. If the physics is indeed controlled by the strong disorder fixed point, then the solutions for different pairs of systems sizes (for the same bare system parameters) should match within error bars. Fig. 3 shows that this is indeed the case. The error bars are created by shifting each value for  $\alpha$  within its error bars, and recalculating  $c$ . To keep the figure clear, we only show the largest and the smallest error bar for each  $\alpha_0$ .

We observe good agreement between the different solutions for  $c$ , and conclude that our system is well described

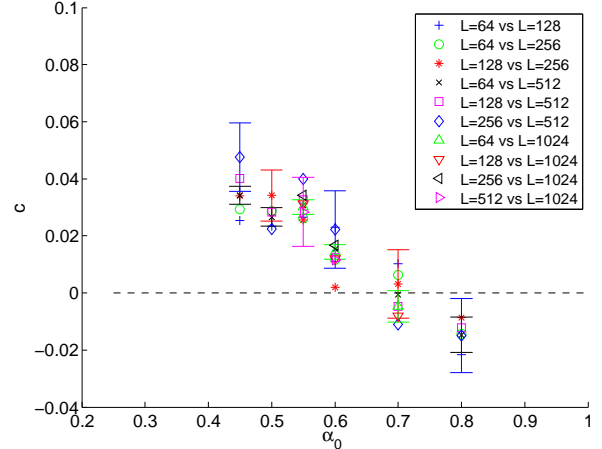


FIG. 3: Solutions of integrated flow equations show good agreement with the strong-disorder fixed point. Solutions  $c$  are plotted for different combination of system sizes as a function of the tuning parameter  $\alpha_0$ . They agree within error bars. Here only the largest and smallest error bars for each  $\alpha_0$  are shown.

by the strong-disorder fixed point. We note that a standard BKT finite-size scaling [17], breaks down and fails to converge for this system [18].

*Conclusions* – We have provided numerical evidence for a novel strong-disorder fixed point of bosons in one dimension. This suggests that the superfluid-to-insulator quantum phase transition changes universality class as the disorder strength is increased: from a BKT-like transition in the case of weak disorder, where the Luttinger parameter becomes universal at the critical point, to a novel kind of phase transition, where the distribution of the superfluid stiffness becomes universal. Our finite-size scaling is quite general and after a slight modification it works also for models without particle-hole symmetry, like the one studied in Ref. 11 (see supplementary information [18]).

It is interesting to note that there is a corresponding transition inside the superfluid phase from a clean superfluid fixed point described by a Luttinger liquid to a disordered superfluid characterized by broad power-law tails in the distribution of  $1/\rho$ . The diverging variance in  $1/\rho$  invalidates the Luttinger liquid description in this regime and leads to the anomalous localization properties discussed in Ref. 19.

The bare disorder distribution used in the numerical simulations were close to the strong-disorder fixed point. It remains to be investigated under what circumstances an arbitrary disorder distribution flows to this novel critical point. A related open question is how the critical behavior changes in the intermediate regime between the weak disorder and strong disorder limits. An intriguing

possibility is that this change is controlled by a new unstable fixed point separating the two regimes.

As our system sizes are finite, it is impossible to formally disprove the conjecture [11] that a truly infinite system will eventually flow to the weak disorder BKT-like transition. But we consider this scenario as highly unlikely, since more weak links are generated as the system size is increased – and they immediately render the system insulating by cutting the chain in parts.

*Acknowledgments*– We thank Lode Pollet, Boris Svistunov, Nikolay Prokof'ev, Daniel Podolsky, Lars Bonnes, Gil Refael, Anatoli Polkovnikov, and Yariv Kafri for illuminating discussions. This work was supported by the ISF, the Minerva foundation, the ERC UQUAM program, the NSF Grant No. PHY11- 25915 during a visit to the KITP-UCSB. E.A thanks the Aspen Center for Physics an NSF Grant #1066293 for hospitality during the writing of this paper. E. A. acknowledges the hospitality of the Miller Institute of Basic Research in Science. S.P. acknowledges support from the Minerva Stiftung. The numerical simulations were carried out on the Weizmann ATLAS Grid cluster and the Weizmann WEXAC cluster.

---

[1] P. C. Hohenberg, Phys. Rev. **158**, 383 (1967).  
[2] N. Mermin and H. Wagner, Phys. Rev. Lett. **17**, 1133 (1966).  
[3] J. M. Kosterlitz and D. J. Thouless, Journal of Physics C: Solid State Physics **6**, 1181 (1973).  
[4] V. L. Berezinskii, Zh. Eksp. Teor. Fiz. **59**, 907 (1970) [Sov. Phys. JETP **32**, 493 (1971)]; V. L. Berezinskii, Zh. Eksp. Teor. Fiz. **61**, 1144 (1971), [Sov. Phys. JETP **34**, 610 (1971).]  
[5] D. R. Nelson and J. M. Kosterlitz, Phys. Rev. Lett. **39**, 1201 (1977).  
[6] J. V. José, L. P. Kadanoff, S. Kirkpatrick, and D. R. Nelson, Phys. Rev. B **16**, 1217 (1977).  
[7] T. Giamarchi and H. J. Schulz, Europhys. Lett. **3**, 1287 (1987).  
[8] E. Altman, Y. Kafri, A. Polkovnikov, and G. Refael, Phys. Rev. Lett. **93**, 150402 (2004).  
[9] E. Altman, Y. Kafri, A. Polkovnikov, and G. Refael, Phys. Rev. B **81**, 16 (2009).  
[10] K. Balabanyan, N. Prokofev, and B. Svistunov, Phys. Rev. Lett. **95**, 2 (2005).  
[11] L. Pollet, N. V. Prokof'ev, and B. V. Svistunov, Phys. Rev. B **87**, 144203 (2013).  
[12] D. Fisher, Phys. Rev. B **50**, 3799 (1994).  
[13] F. Hrahsheh and T. Vojta, Phys. Rev. Lett. **109**, 265303 (2012).  
[14] M. Wallin, E. S. Sørensen, S. M. Girvin, and A. P. Young, Phys. Rev. B **49**, 12115 (1994).  
[15] N. Prokof'ev and B. Svistunov, Phys. Rev. Lett. **87**, 160601 (2001).  
[16] A. Clauset, C. Shalizi, and M. Newman, SIAM Review **51**, 661 (2009).  
[17] H. Weber and P. Minnhagen, Phys. Rev. B **37**, 5986

(1988).

[18] See supplementary material: breakdown of standard BKT finite-size scaling for our model, and review of the strong-disorder RG equations.  
[19] V. Gurarie, G. Refael, and J. Chalker, Phys. Rev. Lett. **101**, 170407 (2008).  
[20]  $\rho_x$  is the stiffness of the one dimensional quantum model. The stiffness of the two dimensional model  $K = \pi\sqrt{\rho_x\rho_\tau}$  defines the Luttinger parameter.  
[21] Only a fraction of the disorder realizations contribute to the tail of the distribution which determines  $\alpha(L)$ . This fraction is smaller near the transition than in the insulator and even smaller deep in the superfluid because less weak links are being generated. Hence more disorder realizations are needed the more we enter into the superfluid.

## SUPPLEMENTARY MATERIAL

### Double-peak structure of the distribution of superfluid stiffness

The superfluid stiffness in Fig. 2a of the main text has a double-peak structure. This is indeed what we expect. We have calculated the superfluid stiffness expected from SDRG by carrying out the RG steps numerically. See Fig. 4 for an example. Here also the double-peak structure is clearly visible. Note that the SDRG operates on the Josephson array model given by Eq. (1) of the main text. This is a different than the current loop model on which the Monte-Carlo calculations are performed. Therefore we do not expect the distributions to match exactly. However the qualitative features of the stiffness distribution are clearly similar, including the power-law tail and the double peak structure.

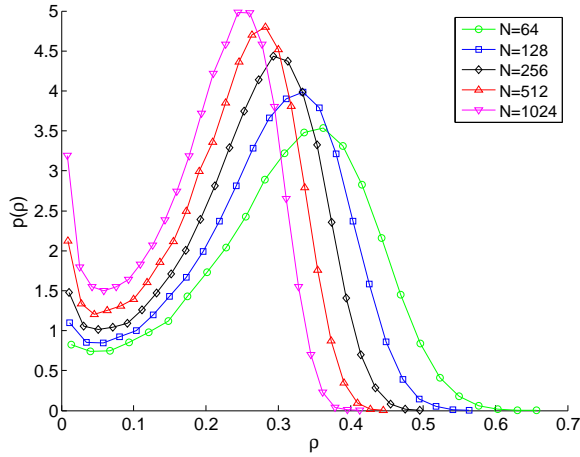


FIG. 4: Distribution of superfluid stiffness obtained by carrying out the SDRG numerically. Here we have used  $d = 200000$  disorder realizations. The initial disorder distribution were the fixed-point distributions with  $u_0 = 0.2$  and  $\alpha_0 = 0.4$ .

### Berezinskii-Kosterlitz-Thouless scaling fails

Here we show that the transition of our model is not described by BKT scaling. Near the critical point of a BKT transition, the Luttinger parameter  $K$  flows as a function of system size  $L$  as

$$K(L) = K_c + \frac{1}{\ln(L) + C} \quad (6)$$

where  $K_c$  is the critical value of the Luttinger parameter at the transition, and  $C$  is a non-universal constant. Following Ref. 17 we treat both  $K_c$  and  $C$  as fitting parameters, and fit our measured values of Luttinger parameter  $K = \pi\sqrt{\rho_x\rho_\tau}$  to Eq. (6). If the transition were in the BKT universality class, then the mean-square error of the fit would have a clear minimum at the phase transition, and the corresponding fitted value of  $K_c$  would be equals 2 at the transition. As shown in Fig. 5 this is not the case.

### Scaling equations for the strong-disorder fixed point

The scaling equations for the parameters  $\alpha$  and  $u$  from SDRG are [8, 9]

$$\frac{du}{d\Gamma} = -\alpha u - (\alpha + 1)u^2 \quad (7a)$$

$$\frac{d\alpha}{d\Gamma} = -b(\alpha + 1)u \quad (7b)$$

Here  $\Omega = \Omega_0 e^{-\Gamma}$  is the energy cutoff. The value of the parameter  $b$  is the only difference between two different disordered models:  $b = 1$  in the particle-hole symmetric case of a commensurate lattice potential at integer filling, and  $b = 1/2$  in case of chemical-potential disorder. These scaling equations are solved to obtain the flow lines  $u(\alpha, b, c)$

$$u(\alpha, b, c) = \frac{1}{b} e^{(\alpha+1)/b} \int_{(\alpha+1)/b}^{1/b} \frac{e^{-t}}{t} dt + e^{\alpha/b} - 1 + c e^{(\alpha+1)/b}.$$

Energy cutoff and renormalized length of the system are related as

$$\frac{dl_\Gamma}{d\Gamma} = l_\Gamma(\alpha + 1 + u) \quad (8)$$

where  $l_\Gamma$  is the average number of original sites per remaining cluster. In integral form these flow equations become

$$-\int_{\alpha_2}^{\alpha_1} \frac{1}{u(\alpha, b, c)} d\alpha - \log\left(\frac{\alpha_1 + 1}{\alpha_2 + 1}\right) + b \log\left(\frac{L_2}{L_1}\right) = 0.$$

For our model we have  $b = 1$ ; with  $b = 1/2$  our finite-size-scaling method also works for models with particle-hole symmetry, as the one studied in Ref. 11.

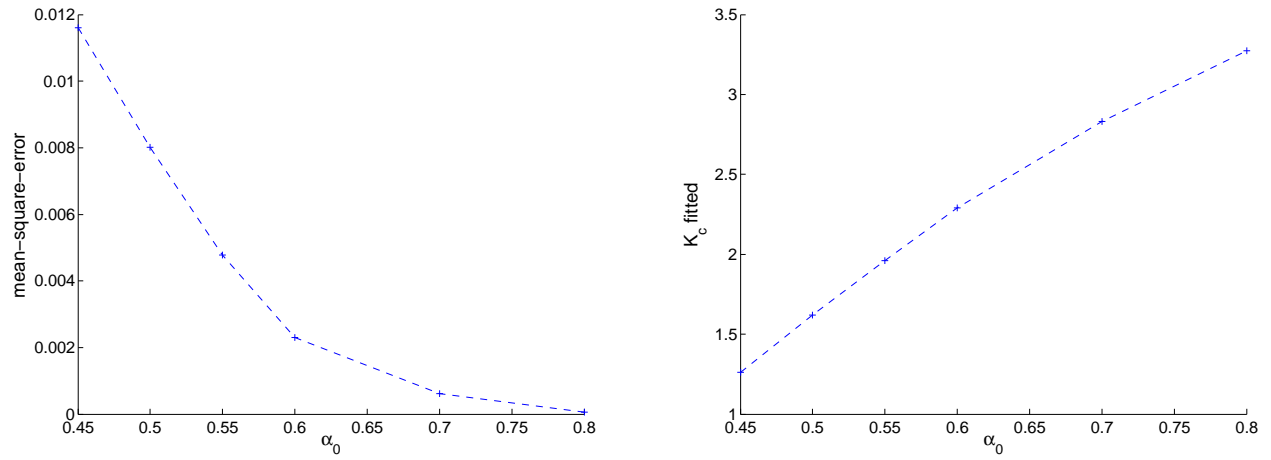


FIG. 5: A standard BKT-scaling procedure, the Weber-Minnhagen fit, fails to locate a BKT phase transition. a) mean-square-error of the fit to Eq. (6) should have a minimum at the transition, but here there is no minimum. b) fitted value for  $K_c$ ; if this transition were in the BKT universality class, then we would find  $K_c = 2$  at the position of the minimum. Even if there might be a minimum for larger  $\alpha_0$ , this would be at a value of the Luttinger parameter  $K > 2$ , and so this rules out the weak-disorder scenario.